Original Article

Blast-Induced Traumatic Brain Injury Triggered by Moderate Intensity Shock Wave Using a Modified Experimental Model of Injury in Mice

Yuan Zhou, Li-Li Wen, Han-Dong Wang, Xiao-Ming Zhou, Jiang Fang, Jian-Hong Zhu, Ke Ding

Department of Neurosurgery, Jinling Hospital, Jinling School of Clinical Medicine, Nanjing Medical University, Jiangsu, Nanjing 210002, China

Abstract

Background: The increasing frequency of explosive injuries has increased interest in blast-induced traumatic brain injury (bTBI). Various shock tube models have been used to study bTBI. Mild-to-moderate explosions are often overlooked because of the slow onset or mildness of the symptoms. However, heavy gas cylinders and large volume chambers in the model may increase the complexity and danger. This study sought to design a modified model to explore the effect of moderate explosion on brain injury in mice.

Methods: Pathology scoring system (PSS) was used to distinguish the graded intensity by the modified model. A total of 160 mice were randomly divided into control, sham, and bTBI groups with different time points. The clinical features, imaging features, neurobehavior, and neuropathology were detected after moderate explosion. One-way analysis of variance followed by Fisher's least significant difference posttest or Dunnett's t 3-test was performed for data analyses.

Results: PSS of mild, moderate, and severe explosion was 13.4 ± 2.2, 32.6 ± 2.7 (t = 13.92, P < 0.001; vs. mild group), and 56.6 ± 2.8 (t = 31.37, P < 0.001; vs. mild group), respectively. After moderate explosion, mice showed varied symptoms of malaise, anorexia, incontinence, apnea, or seizure. After bTBI, brain edema reached the highest peak at day 3 (82.5% ± 2.1% vs. 73.8% ± 0.6%, t = 7.76, P < 0.001), while the most serious neurological outcomes occurred at day 1 (Y-maze: 8.25 ± 2.36 vs. 20.00 ± 4.55, t = −4.59, P = 0.048; 29.58% ± 2.84% vs. 49.09% ± 11.63%, t = −3.08, P = 0.008; neurologic severity score: 2.50 ± 0.58 vs. 0.00 ± 0.00, t = 8.65, P = 0.016). We also found that apoptotic neurons (52.76% ± 1.99% vs. 1.30% ± 0.11%, t = 57.20, P < 0.001) and gliosis (2.98 ± 0.24 vs. 1.00 ± 0.00, t = 14.42, P = 0.021) in the frontal were significantly higher at day 3 post-bTBI than sham bTBI.

Conclusions: We provide a reliable, reproducible bTBI model in mice that can produce a graded explosive waveform similar to the free-field shock wave in a controlled laboratory environment. Moderate explosion can trigger mild-to-moderate blast damage of the brain.

Key words: Blast-Induced Traumatic Brain Injury; Brain Edema; Gliosis; Shock Tube; Subarachnoid Hemorrhage

Introduction

Since World War II, explosive weapons have gradually become the main lethal weapons of modern warfare and terrorist activities, and thousands of people worldwide have experienced a blast-induced traumatic brain injury (bTBI).[1,2] Furthermore, increasing numbers of civilians suffer this trauma in ongoing terrorist attacks.[3,4] However, the damage accrued from mild-to-moderate explosions is often overlooked because of the slow onset or mildness of the symptoms.

Research in blast-induced neurotrauma (BINT) has resulted in considerable progress in the past decade.[5-8] Primary shock waves may play a major role in the formation of pathophysiological characteristics that differ from common traumatic brain injury (TBI).[9,10] Appropriate experimental methods are crucial in addressing the biological effects of the primary blast wave. The most common methods are open field exposure, blast tubes for explosive damage, and shock tubes with compressed air or gas.[11] The third

Access this article online

Quick Response Code:

Website: www.cmj.org

DOI: 10.4103/0366-6999.243558

Address for correspondence: Prof. Han-Dong Wang, Department of Neurosurgery, Jinling Hospital, Jinling School of Clinical Medicine, Nanjing Medical University, Jiangsu, Nanjing 210002, China
E-Mail: njhdwang@hotmail.com

Received: 13-07-2018 **Edited by:** Qiang Shi

How to cite this article: Zhou Y, Wen LL, Wang HD, Zhou XM, Fang J, Zhu JH, Ding K. Blast-Induced Traumatic Brain Injury Triggered by Moderate Intensity Shock Wave Using a Modified Experimental Model of Injury in Mice. Chin Med J 2018;131:2447-60.

model has been frequently used because of its single shock wave factor without other injury mechanisms.[12] Sophisticated shock tube systems have been installed at the Walter Reed Institute, the United States Naval Medical Research Center, the Applied Physics Laboratory at Johns Hopkins University, and other institutions.[11,13-15] A novel methodology that subjects BINT models to excess pressures *in vivo* and *in vitro* through a drive chamber consisting of a flange connection has been reported.[16] However, heavy gas cylinder and large volume chambers in the model may increase the complexity and danger of operation. To optimize these issues, we have designed a modified shock tube system and explored the effect of moderate explosion on brain injury in mice.

Methods

Ethical approval

All procedures were approved by the Animal Care and Use Committee of Nanjing Medical University and were conducted in accordance with the Animals Research: Reporting *In Vivo* Experiments guidelines.

Animals

Male imprinting control region (ICR) mice (28–32 g, 7–8 weeks of age) were purchased from the Experiment Animal Center of Jinling Hospital, Jiangsu, China. The mice were housed using a 12 h light/dark cycle at 23 ± 1°C with free access to food and water and were acclimatized for at least 2 days before any experiment.

Design of blast model

A modified shock tube system [Figure 1] was built to provide a range of blast conditions according to the prior descriptions.[16] The driver section consisted of a 17-mm-thick spacer flange (stainless steel) bolted together with a corresponding blind flange. The flange was welded to the driver pipe. Full-faced gaskets (Buna-N material) were installed between each flange to prevent leakage. The diaphragm composed of a polytetrafluoroethylene (PTFE; JVS, Shenzhen, China) film was installed between the driver spacer flange and the flange attached to the driver section. An electric gas pump (Jumu, Wuhan, China) with an explosion-proof tube provided high-pressure air to the driver section through a fitting on the back of the blind flange. A pressure meter located in the driver section (PS0) was used to measure the burst pressure at the rupture of the PTFE film. The driver section (length: 750 mm, diameter: 74 mm) was an open-end round stainless steel pipe with three side holes coupled to three high-frequency dynamic pressure transmitters (Aire Sensor Technology Co., Nanjing, China). The pressure sensor located next to the mouse 660 mm downstream from the membrane (PS3) was used to classify blast severity, while the other pressure sensors (PS1 and PS2) located 160 mm and 410 mm downstream from the membrane, respectively, were used to monitor the blast duration and the velocity of the pressure pulse. All sensor data were collected at a frequency of 20 kHz, and the data were sent to a computer through the multichannel acquisition and supporting software (Aire Sensor Technology Co., Nanjing, China). The shock tube system was mounted horizontally on a machined stainless steel frame. The animal holder was a metal mesh fixture that could be placed inside the driven section of the shock tube.

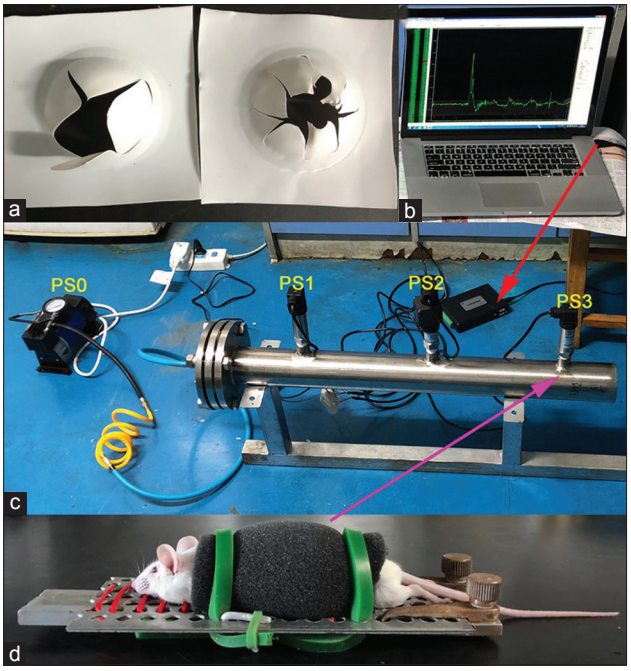

Figure 1: A modified shock tube system. (a) The frontal view of the ruptured PTFE films. (b) All sensor data were sent to the computer (red arrow) through the multichannel acquisition. (c) The main part of the model comprised the driver and the driven section, separated by a PTFE film. The driven chamber had three side holes coupled to three high-frequency dynamic pressure transmitters (PS1, PS2, and PS3). The compressed air produced by our electric gas pump was monitored by another pressure meter PS0. The shock tube system was mounted horizontally on a machined stainless steel frame. (d) The anesthetized mouse was mounted in prone position to the animal holder. The holder positioned the mouse with torso shielding at PS3 inside the pipe (purple arrow). PTFE: Polytetrafluoroethylene.

Blast exposure

Before each test, all metal threaded connections were required to be sealed and checked for parallel leaks. Then, an intact PTFE film was inserted between the two sections to create a closed volume driver section that would allow pressurization. Next, the mouse was anesthetized with an intraperitoneal injection of chloral hydrate (1%, 5 ml/kg; Aladdin, Shanghai, China) and then mounted in the prone position on the animal holder. The head, neck, torso with torso shielding, and abdomen of the mouse were fixed to the holder aiming to avoid any movement. The forehead faced the direction of the shock wave flow. The holder positioned the mouse at PS3 in the pipe, ensuring that only a well-formed incident shock wave loaded the mouse and potential rarefactions from the tube opening were minimized. Increase of driver chamber pressure by compressed air eventually led to the rupture of PTFE film when it exceeded the force threshold of the membrane. At that time, high-pressure airflow would rush

to the outlet of the driver tube section, and the shock waves with different peaks could be generated owing to film of varying thickness (0.1–0.8 mm). Atmospheric temperature, pressure, and humidity were consistent in each test. Pressure and duration of different positions were recorded for every procedure by the software.

Blast injury severity and mortality

Based on different peak incident pressures produced by films of varied thickness from previous literature, the mice (n = 120) were divided into three groups (mild, moderate, and severe intensity shock wave; n = 40 per group) by simple randomization.[13,17] Once basic reflexes were restored, the mice were returned to the home cage with free access to food and water. The mortality rate was assessed 24 h postblast injury. Blast injury severity in animals was determined using a slightly modified pathology scoring system (PSS) for blast injuries.[18] Intergroup consistency was performed on PSS of graded blast injury.

Groups

A total of 160 mice were divided into eight groups (n = 20 per group) by simple randomization: control, sham bTBI, and six bTBI groups (6 h, 1 day, 2 days, 3 days, 7 days, and 14 days). Among them, the mice in the bTBI 2-day group were only used for neurological evaluation and blood-brain barrier (BBB) permeability. After the same anesthesia, the sham group animals heard the explosion but were not subjected to the blast shock wave. The control group just experienced the same anesthesia.

Clinical features and computed tomography

Clinical manifestations of injury in the 100 mice induced by moderate explosion were observed 24 h after the blast using computed tomography (CT) scans. Twenty sham mice were also examined. CT imaging was done using a CereTom X-ray CT Scanner system (NeuroLogica Corp., Danvers, MA, USA). Dicom files of CT images were evaluated by CereTom™ WS software (NeuroLogica Corp., Danvers, MA, USA).

Neurological evaluation

The neurologic status was evaluated using a modified 10-point neurological severity score (NSS).[19] Two investigators who were blinded to the experimental groups evaluated the ability of each mouse to perform 10 different tasks that demonstrated motor function, balance, and alertness. One point was given for failure to perform each of the tasks [Table 1].

Righting reflex response was evaluated as an indicator of neurologic restoration. Immediately following bTBI, the mice were placed on their backs in a clean cage. The time taken to adopt a prone position following bTBI or anesthesia was recorded by three observers blinded to the treatment. The three time values were averaged for a single value for each subject.[20]

Spatial recognition memory and motor activity were carried out in a previously described two-trial Y-maze.[21] In each trial, the mice were placed onto the end of one arm and allowed to explore freely for 5 min. The start position for each trial was kept constant for the same animal, but was changed to a different arm between mice. The number of arms visited and time spent in each arm were recorded. During trial 1, one of the arms was blocked, allowing for the exploration of only two arms. After a 30-min delay, trial 2 was conducted in which all three arms became available for exploration. All the mice were acclimated to the test room for 30 min before experimentation using this and all other behavioral assays.

Table 1: Modified neurologic severity score

Task	Points (success/failure)
Exit a circle of 30-cm diameter within 3 min	0/1
Paresis of upper and/or lower limbs of one lateral side	0/1
Able to walk straight	0/1
Presence of the startle reflex	0/1
Presence of seeking behavior	0/1
Able to balance on a beam of 7-mm width for 10 s	0/1
Able to balance on a round stick of 5-mm diameter for 10 s	0/1
Able to cross a 30-cm-long beam of 3 cm width	0/1
Able to cross a 30-cm-long beam of 2 cm width	0/1
Able to cross a 30-cm-long beam of 1 cm width	0/1
Maximum total	10

Brain water content

Brain water content was performed as described previously.[22] Briefly, the brain was removed from each mouse and placed on a cooled brain matrix 1 day after treatment. The brain cerebellum and stem were excised, and the rest of the tissue was weighed immediately to obtain wet weight (ww). Subsequently, the tissue was dried at 80°C for 72 h and weighed to obtain dry weight (dw). The brain water content (%) was calculated as (ww − dw)/ww × 100.

Blood-brain barrier permeability

BBB permeability was quantified by the 2% Evans blue (EB) dye extravasation method.[23] Briefly, all mice were intravenously injected with 4 ml/kg of 2% EB 1 h before each mouse was killed [Figure 2b]. The mice were anesthetized and perfusion was performed through the left ventricle with phosphate-buffered saline to remove the intravascular EB dye. This was continued until the fluid from the right atrium turned colorless. Cortex samples were collected, mixed with 50% trichloroacetic acid, and centrifuged. The absorbance of the supernatant was measured at 620 nm using a multifunctional enzyme labeling instrument (Molecular Devices, Sunnyvale, CA, USA).

Tissue processing

Mice in the different groups were deeply anesthetized with chloral hydrate and perfused intracardially with 30–40 ml of cold (4°C) heparinized 0.9% saline. For immunohistochemistry and hematoxylin and eosin

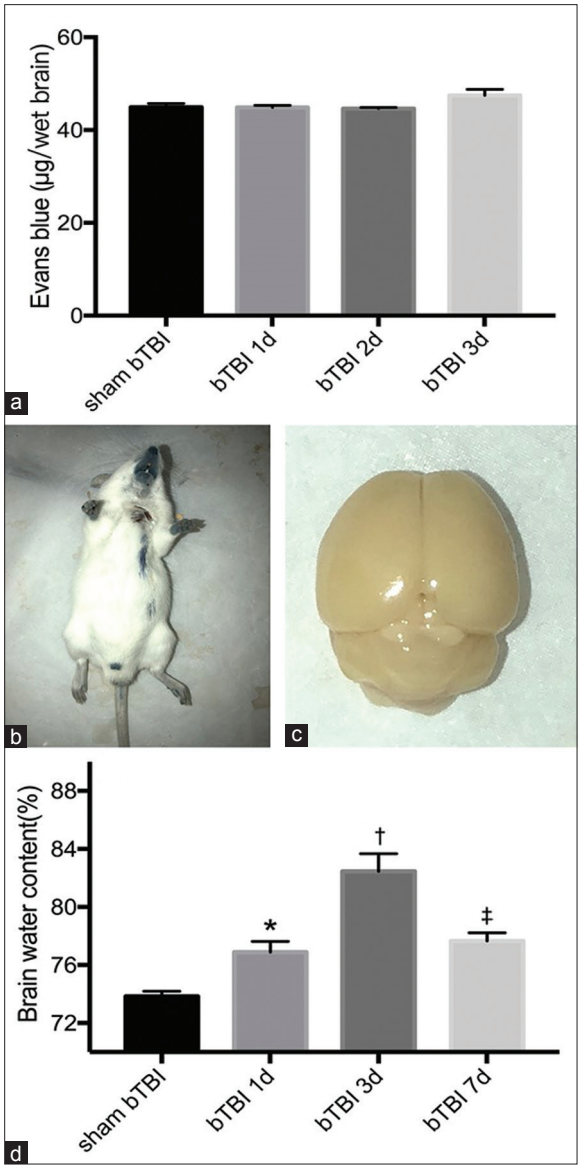

Figure 2: The BBB permeability and brain water content after bTBI induced by moderate intensity shock wave. (a) No significant difference was found in the amount of Evans blue dye among sham bTBI (44.9 ± 0.8 μg/wet brain), bTBI 1-day (44.9 ± 0.4 μg/wet brain, $t = -0.06$, $P > 0.05$), bTBI 2-day (44.6 ± 0.3 μg/wet brain, $t = -0.68$, $P > 0.05$), and bTBI 3-day groups (47.5 ± 1.3 μg/wet brain, $t = 2.89$, $P > 0.05$), indicating little discrepancy of the BBB. (b) One representative mouse in bTBI group was injected with 4 ml/kg of 2% Evans blue intravenously. (c) The representative whole brain dissected after bTBI showed no significant blue dye. (d) After bTBI induced by moderate intensity shock wave, the degree of brain edema increased significantly at 1 day (76.9% ± 1.3% vs. 73.8% ± 0.6%, $t = 2.75$, $P = 0.025$), reached the highest peak at 3 days (82.5% ± 2.1% vs. 73.8% ±0.6%, $t = 7.76$, $P < 0.001$), and decreased slightly but remained higher at 7 days than that of the sham bTBI group (77.7% ± 1.0% vs. 73.8% ± 0.6%, $t = 3.44$, $P = 0.009$). Data were presented as the mean ± standard error of the mean ($n = 6$ in each group). *$P < 0.05$, †$P < 0.001$, ‡$P < 0.01$ compared with sham bTBI group. BBB: Blood–brain barrier; bTBI: Blast-induced traumatic brain injury.

(H and E) staining, the mice were perfused with the same saline formulation followed by 20–30 ml of cold 4% paraformaldehyde. The entire brain was removed and immersed in 4% paraformaldehyde overnight. For immunofluorescence, the brain was subsequently immersed in 20% sucrose followed by 30% sucrose.

Gross observation and hematoxylin and eosin stain

Sham- and blast-exposed mice were euthanized for standard gross assessment at 6 h postblast. The whole brain and the coronal sections were viewed for contusion, hematoma, edema, or subarachnoid hemorrhage.

Brain-tissue samples were obtained, embedded in paraffin, and cut coronally into sections 6 μm thick. The sections in the frontal lobe and hippocampus were stained with H and E and examined by light microscopy by a pathologist blinded to the animal status. Six simple random high-power vision fields in each coronary section were chosen, and the mean number of necrotic cells was determined in each section. A total of four sections from each animal were used for quantification. The final average number of the four sections was regarded as the data for each sample.

Immunofluorescence staining

For immunofluorescence, serial 8 μm coronal sections were obtained using a cryostat. Four sets of five sections including the frontal cortex and hippocampus were collected from each brain. Based on the established immunostaining protocol, the slides were incubated in blocking buffer comprised 10% normal goat serum in phosphate-buffered saline (PBS) containing 0.1% Triton X-100 for 2 h followed by overnight incubation at 4°C in primary antibody. The primary antibodies used were mouse anti-glial fibrillary acidic protein (GFAP, 1:200 dilution; eBioscience, San Diego, CA, USA) and mouse anti-neuronal nuclei (NeuN, 1:100 dilution; Millipore, Bedford, MA, USA). The next day, the slides were washed three times with PBS for 5 min each time and then incubated with appropriate secondary antibody for 1 h at room temperature. The mouse anti-NeuN secondary antibody was incubated with terminal deoxynucleotidyl transferase-mediated dUTP nick 3'-end labeling (TUNEL) compound for 1 h at 37°C. The slides were washed three times in PBS, counterstained with 4',6-diamidino-2-phenylindole (DAPI; Beyotime Biotech Inc., Nantong, China) for 2 min and rinsed with PBS. Coverslips were applied with mounting medium. Fluorescence was imaged on an IX71 inverted microscope system (Olympus, Tokyo, Japan) and analyzed using Image-Pro Plus 6.0 software (Media Cybernetics, Silver Spring, MD, USA). The specificity of the immunofluorescence reaction was evaluated by replacing the primary antibody with PBS.

TUNEL was performed to detect dying cells in the frontal lobe using an *in situ* Cell Detection Kit (Roche, South San Francisco, CA, USA) according to the manufacturer's instructions. The ratio of the number of apoptosis cells to DAPI was determined as the apoptosis index, while the number of apoptosis neurons was determined by the ratio of apoptosis cells to neurons. Six simple random vision

fields (×200) in each coronary section were chosen, and the mean apoptosis index or the apoptotic ratio of the total neurons in the six views were regarded as the data of each section.[24,25] A total of four sections from each animal were used for quantification. The final average number of the four sections was regarded as the data for each sample. Data were presented per ×200 magnification field. All procedures were performed by two investigators who were blind to the experimental groups.

Immunohistochemistry

Serial sections (4 μm) were cut coronally through the cerebrum and routinely deparaffinized. Endogenous peroxidase was blocked with 3% hydrogen peroxide/methanol. Nonspecific antibody binding was blocked by incubating the sections in blocking buffer comprised 10% normal goat serum in PBS for 30 min. Primary antibody (rabbit anti-GFAP, 1:1000 dilution; Abcam, Cambridge, MA, USA) was applied overnight at 4°C. After being washed three times in PBS for 5 min each time, the sections were treated according to the instructions of the EliVision Plus Kit (MXB Biotechnologies, Fujian, CHINA) to visualize GFAP. Six simple random high-power fields (500×) in each coronary section were chosen, and the mean integrated optical density (IOD) of GFAP positive areas was regarded as the data of each section. A total of four sections from each animal were used for quantification. The final average number of the four sections was regarded as the data for each sample. Data were presented as the ratio of mean IOD of different bTBI group to sham bTBI group per high-power field. All the processes were conducted using Image-Pro Plus software (Media Cybernetics, Silver Springs, MD, USA) by two investigators blinded to the grouping.

Statistical analysis

SPSS 24.0 software (IBM Corp., Armonk, NY, USA) was used for the statistical analyses. Each experiment was repeated at least three times. One-way analysis of variance (ANOVA) followed by Fisher's LSD posttest or Dunnett's t 3-test based on the homogeneity of variance was performed for data analyses. Significance was assigned at $P < 0.05$.

Results

Characterization of the shock tube

Pressure time histories recorded at PS2 and PS3 were concordant with a typical Friedlander wave [Figure 3a and 3b]. At PS3, the measured shock wave speed increased with blast pressure and was close to the calculated theoretical shock wave speed based on one-dimensional shock tube theory [Figure 3c]. The duration of blast peak incident pressures at PS3 was 3.24 ± 0.58 ms. Graded blast [Figure 3d] indicated that peak incident pressures were linearly and positively related to the duration of the explosion ($F = 103.14$, $P < 0.001$; $F = 50.45$, $P < 0.001$; $F = 51.93$, $P < 0.001$), respectively. In all the blasts, the rupture patterns of the shock tube diaphragm membranes were basically consistent.

Blast injury severity and mortality

Graded shock wave intensity determined by different peak incident pressures corresponded to discrepant PSS and mortality. In mild intensity shock wave, the peak incident pressure of 170 ± 14 kPa at P3 produced 13.4 ± 2.2 PSS and no lethality (0/40). PSS and mortality of blast injury severity in mice were 32.6 ± 2.7 ($t = 13.92$, $P < 0.001$) and 5% (2/40) after moderate intensity blast (236 ± 24 kPa at P3, $t = 6.99$, $P < 0.001$), respectively, but were 56.6 ± 2.8 ($t = 31.37$, $P < 0.001$) and 20% (8/40) after severe intensity blast (330 ± 27 kPa at P3 $t = 17.01$, $P < 0.001$) [Figure 3e]. The data demonstrated the intergroup consistency and repeatability. The most varied damage was observed in the lungs [Table 2], which had been used for classification. Death occurred mostly due to severe lung damage or imminent cardiorespiratory arrest.

Clinical presentation, computed tomography imaging, and gross observation after blast-induced traumatic brain injury induced by moderate intensity shock wave

After bTBI induced by moderate blast, the mice showed varied symptoms of malaise (90/100, 90%), anorexia (85/100, 85%), apnea (5/100, 5%), seizure (5/100, 5%), and incontinence (35/100, 35%). Anorexia was defined as the loss of the desire to eat, while seizure was characterized by wet dog shakes, and clonus of the face, head, and limbs. CT images of sham bTBI mice showed no signs of hemorrhage, contusion, or subarachnoid hemorrhage [Figure 4a-4c]. Subarachnoid hemorrhage [Figure 4d-4f] on the film appeared obviously in 95% (19/20) mice 6 h post-bTBI, was not evident in one mouse (5%) mice 1 day post-bTBI, and had disappeared in mice in the other blast groups.

Gross observation of the whole brains following bTBI induced by moderate blast showed brain edema without focal lesions, contusion, or subarachnoid hemorrhage [Figure 5b]. However, subarachnoid hemorrhage was observed in some coronal sections [Figure 5d]. Neither the whole brain nor the coronal sections in the sham bTBI group showed edema or bleeding [Figure 5a and 5c].

Most serious neurological outcomes occurred 1 day after blast-induced traumatic brain injury induced by moderate intensity shock wave

Figure 6 displays the neurological outcomes after bTBI induced by moderate blast. The response to spatial memory and motor activity was tested in a Y-maze procedure. During the first trial, the total number of visits was reduced significantly in bTBI at 1 day [Figure 6a; 10.75 ± 1.26 vs. 19.75 ± 4.86, $t = -3.49$, $P = 0.003$] and bTBI at 7 days (10.75 ± 2.99 vs. 19.75 ± 4.86, $t = -3.49$, $P = 0.003$). However, there was no difference in spatial preference [Figure 6b]. During the second trial of the Y-maze, the total number of visits in the bTBI 1-day group decreased significantly [Figure 6c, 8.25 ± 2.36 vs. 20.00 ± 4.55, $t = -4.59$, $P = 0.048$]. The measure of spatial recognition memory and novel-arm preference detected significant differences in the bTBI 1-day group [Figure 6d; 29.58% ± 2.84% vs. 49.09% ± 11.63%, $t = -3.08$, $P = 0.008$] and bTBI 6-h group (34.75% ± 6.02%

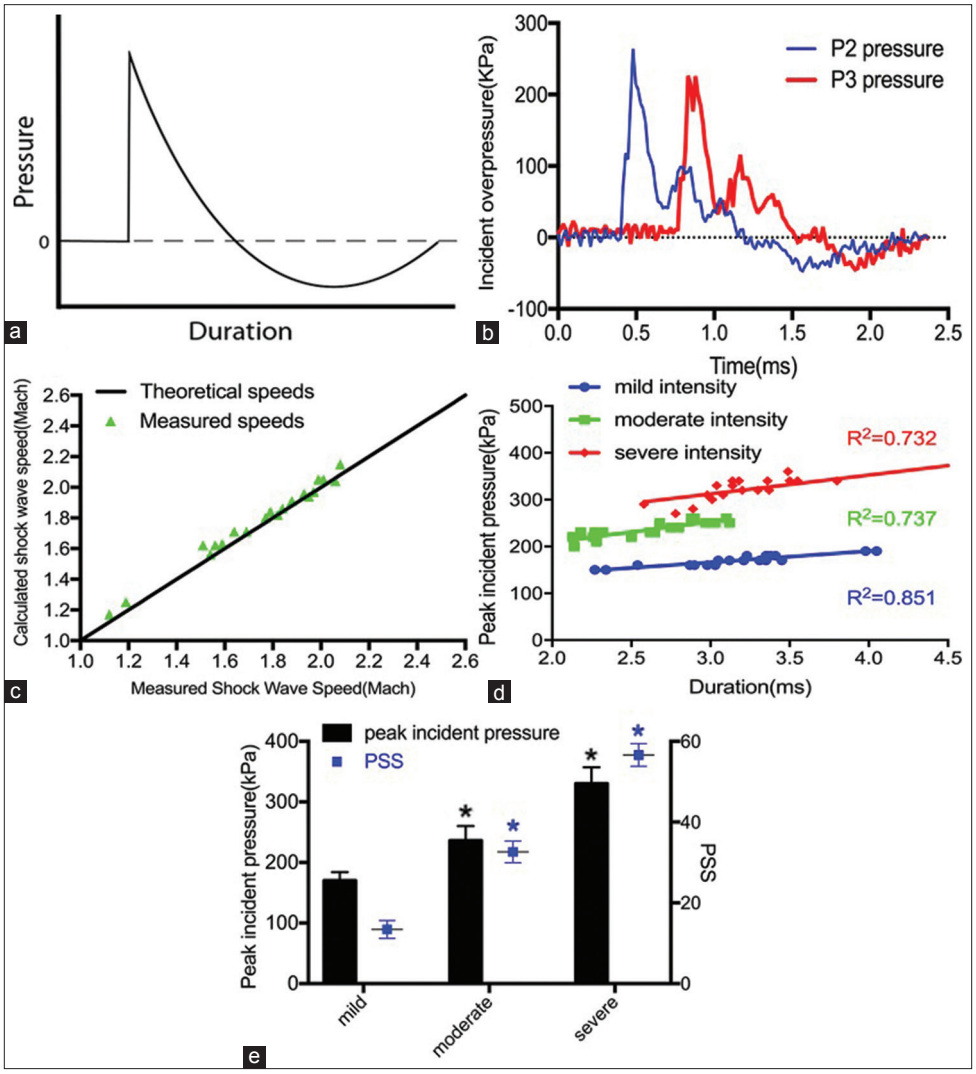

Figure 3: Characterization of the shock tube. (a) A typical Friedlander wave of pressure time history. (b) Pressure time histories recorded at PS2 (blue) and PS3 (red) during one moderate intensity explosion were concordant with a typical Friedlander wave and had a little time interval. The duration of blast peak incident pressures at PS3 was 3.24 ± 0.58 ms. (c) The shock wave speed measured at PS3 (green triangle) matched the theoretical speeds (black straight line) at PS3 for a developed shock wave induced by moderate blast. (d) Peak incident pressures duration diagram at PS3. In mild (blue, $R^2 = 0.851$), moderate (green, $R^2 = 0.737$), and severe (red, $R^2 = 0.732$) intensity blasts, peak incident pressures were linearly and positively related to the duration of the explosion ($F = 103.14$, $P < 0.001$; $F = 50.45$, $P < 0.001$; $F = 51.93$, $P < 0.001$), respectively. (e) Graded shock wave intensity determined by different peak incident pressures corresponded to discrepant PSS (blue). In mild intensity shock wave, the peak incident pressure of 170 ± 14 kPa at P3 produced 13.4 ± 2.2 PSS. PSS of blast injury severity in mice was 32.6 ± 2.7 ($t = 13.92$, $P < 0.001$) after moderate intensity blast (236 ± 24 kPa at P3, $t = 6.99$, $P < 0.001$), while 56.6 ± 2.8 ($t = 31.37$, $P < 0.001$) after severe intensity blast (330 ± 27 kPa at P3, $t = 17.01$, $P < 0.001$). Data were presented as the mean ± standard error of the mean ($n = 40$ in each group). *$P < 0.001$ compared with mild intensity blast group. PSS: Pathology scoring system.

vs. 49.09% ± 11.63%, $t = -2.26$, $P = 0.039$). Novel-arm preference for the new arm in the second trial was at a 33% chance level. The data suggest that the damage to spatial memory and motor activity was the most severe at 1 day after bTBI. The NSS of both the control and sham bTBI groups was zero [Figure 6e]. Although the NSS 6 h after bTBI rose, the increase was not significant. Mice at 24 h after bTBI showed the worst performance (2.50 ± 0.58, $t = 8.65$, $P = 0.016$). The NSS at 2 days after bTBI returned to zero. The results of righting reflex [Figure 6f] showed that moderate blast impact increased the recovery time (320.83 ± 166.27 s vs. 50.00 ± 22.58 s, $t = 3.95$, $P = 0.027$).

Brain edema, not BBB permeability, was the most significant at 3 days after blast-induced traumatic brain injury induced by moderate intensity shock wave

No significant difference was found in the amount of EB dye among sham bTBI [Figure 2a; 44.9 ± 0.8 μg/wet brain], bTBI 1 day (44.9 ± 0.4 μg/wet brain, $t = -0.06$, $P > 0.05$), bTBI 2 days (44.6 ± 0.3 μg/wet brain, $t = -0.68$, $P > 0.05$), and bTBI 3-day groups (47.5 ± 1.3 μg/wet brain, $t = 2.89$, $P > 0.05$), indicating little discrepancy of the BBB. The whole brain dissected after bTBI showed no significant blue dye [Figure 2c].

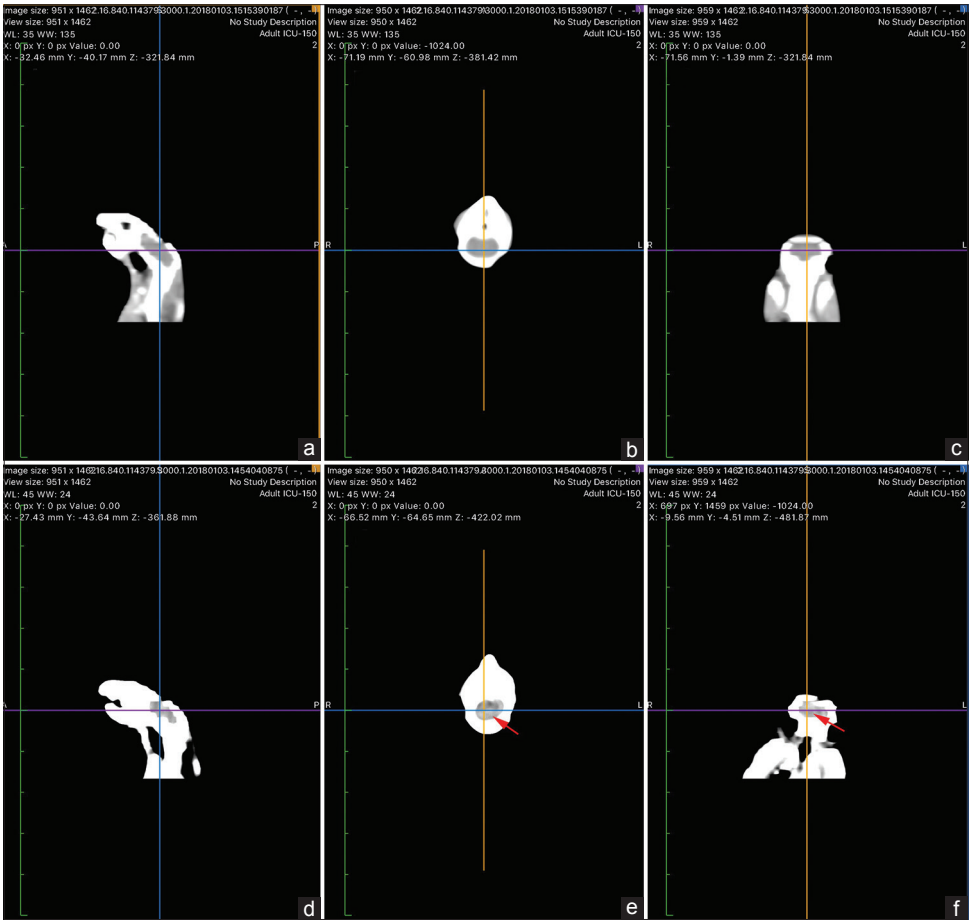

Figure 4: Head CT scans. (a-c) CT images of one sham bTBI mouse showed no signs of hemorrhage, contusion, or subarachnoid hemorrhage. (d-f) Subarachnoid hemorrhage (red arrows) was observed in one mouse 6 h post bTBI on the film. CT: Computed tomography; bTBI: Blast-induced traumatic brain injury.

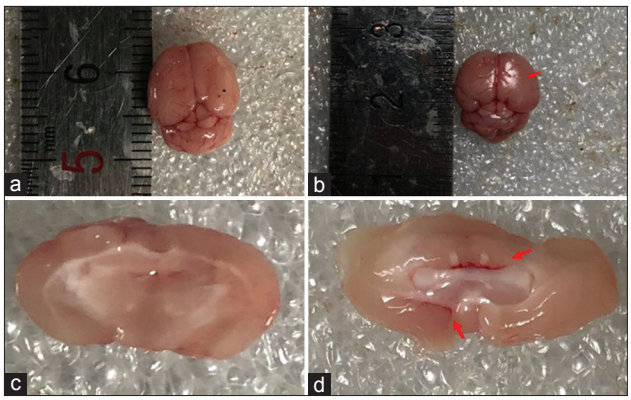

Figure 5: Gross pathological observation of the brains. Neither the whole brain (a) nor the coronal section (c) in sham bTBI group showed edema or bleeding. (b) The whole brains following bTBI induced by moderate intensity shock wave showed brain edema without focal lesions, contusion, or subarachnoid hemorrhage. Red arrow indicates the brain edema. (d) Subarachnoid hemorrhage (red arrows) was observed inside partial of the coronal section in bTBI group. bTBI: Blast-induced traumatic brain injury.

As shown in Figure 2d, after bTBI was induced by moderate explosion, the degree of brain edema increased significantly at 1 day (76.9% ± 1.3% vs. 73.8% ± 0.6%, $t = 2.75$, $P = 0.025$), reached the highest peak at 3 days (82.5% ± 2.1% vs. 73.8% ± 0.6%, $t = 7.76$, $P < 0.001$), and decreased slightly but remained higher at 7 days than that of the sham bTBI group (77.7% ± 1.0% vs. 73.8% ± 0.6%, $t = 3.44$, $P = 0.009$).

Hematoxylin and eosin stain reveals the most necrotic cells in the frontal lobe and hippocampus 3 days after blast-induced traumatic brain injury induced by moderate intensity shock wave

H and E staining of sections reflected the extent of injury. The most significant necrotic cells were visible at 3 days (78 ± 8/high-power field [HPF] vs. 2 ± 1/HPF, $t = 6.1$, $P < 0.001$) after bTBI in the frontal lobe [Figure 7]. The bTBI 3-day group displayed more necrotic cells in CA1 and CA3 regions [Figure 8; 50 ± 5/HPF, $t = 16.3$, $P < 0.001$ and 40 ± 4/HPF, $t = 21.1$, $P < 0.001$] of the hippocampus than the sham group (5 ± 2/HPF, and 2 ± 1/HPF).

Apoptotic cells and neurons are increased significantly in the frontal lobe of blast-induced traumatic brain injury at 3 days

As shown in Figure 9, double staining of TUNEL

Table 2: Number of graded bTBI mice partitioned into observed injury categories (n = 120)

Organ	PSS grade				
	Negative (0)	Trace (1–4)	Mild (5–21)	Moderate (22–36)	Severe (37–64)
Lung	3	0	39	38	40
Pharynx/larynx	120	0	0	0	0
Trachea	120	0	0	0	0
Hollow abdominal organs*	118	0	1	1	0
Solid abdominal organs†	120	0	0	0	0

*Small intestine, large colon, small colon, cecum, rectum, gall bladder, and urinary bladder; †Liver, spleen, pancreas, adrenals, and kidneys. bTBI: Blast-induced traumatic brain injury; PSS: Pathology scoring system.

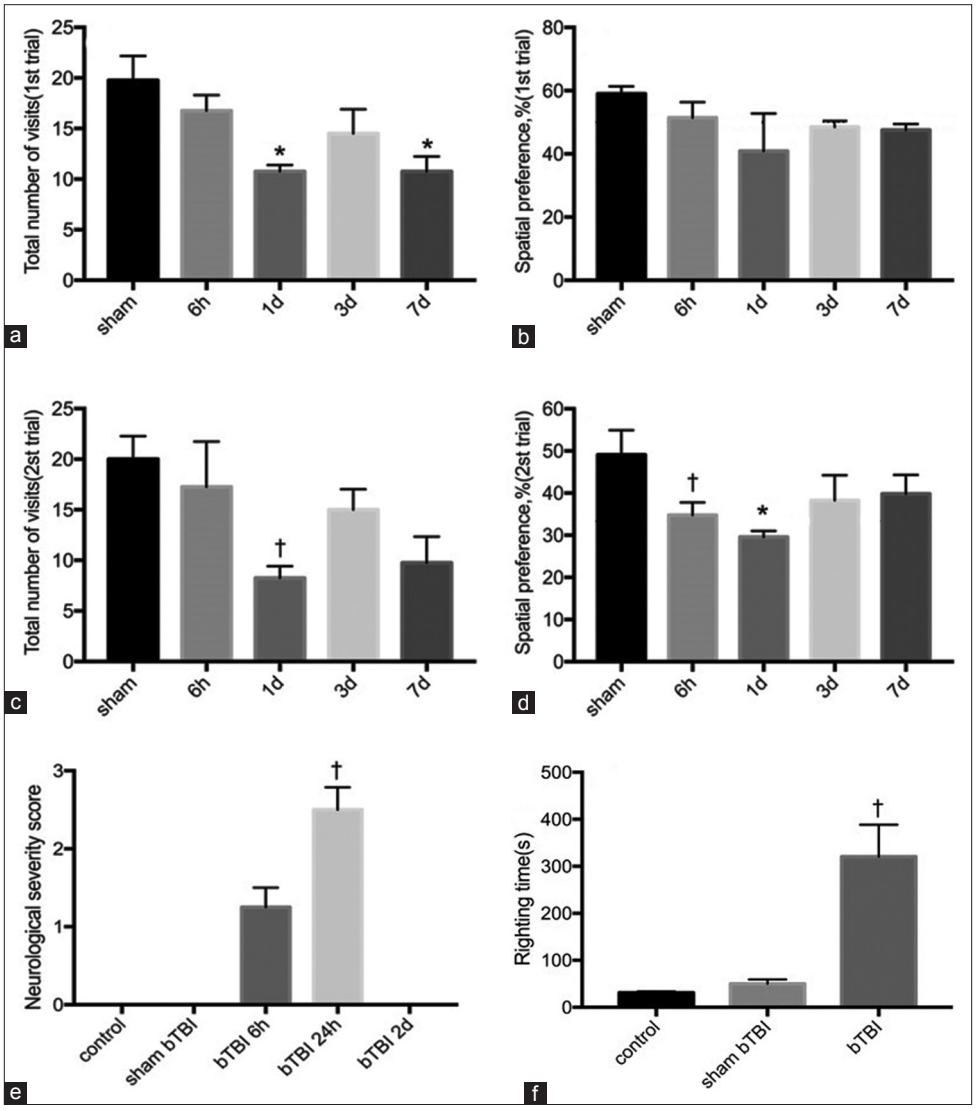

Figure 6: The neurological outcome using a Y-maze, modified NSS, and recovery of righting reflex. (a) During the first trial of Y-maze, total number of visits was reduced significantly in bTBI at 1 day (10.75 ± 1.26 vs. 19.75 ± 4.86, $t = -3.49$, $P = 0.003$) and bTBI at 7 days (10.75 ± 2.99 vs. 19.75 ± 4.86, $t = -3.49$, $P = 0.003$). (b) During the first trial of Y-maze, mice of all groups spent approximately similar time in one of the two arms. (c) During the second trial of the Y-maze, the total number of visits in the bTBI 1-day group decreased significantly (8.25 ± 2.36 vs. 20.00 ± 4.55, $t = -4.59$, $P = 0.048$). (d) During the second trial of Y-maze, the measure of spatial recognition memory and novel-arm preference detected a significant differences in the bTBI 1-day group (29.58% ± 2.84% vs. 49.09 ± 11.63%, $t = -3.08$, $P = 0.008$) and bTBI 6-h group (34.75% ± 6.02% vs. 49.09% ± 11.63%, $t = -2.26$, $P = 0.039$). (e) The NSS of both the control and sham bTBI groups was zero. Although the NSS at 6 h after bTBI rose, the increase was not significant. Mice at 24 h after bTBI showed the worst performance (2.50 ± 0.58, $t = 8.65$, $P = 0.016$). The NSS at 2 days after bTBI returned to zero. (f) The moderate blast increased the recovery time (320.83 ± 166.27 s vs. 50.00 ± 22.58 s, $t = 3.95$, $P = 0.027$). Data were presented as the mean ± standard error of the mean (n = 10 in each group). *$P < 0.01$, †$P < 0.05$ compared with sham bTBI group. bTBI: Blast-induced traumatic brain injury; NSS: Neurological severity score.

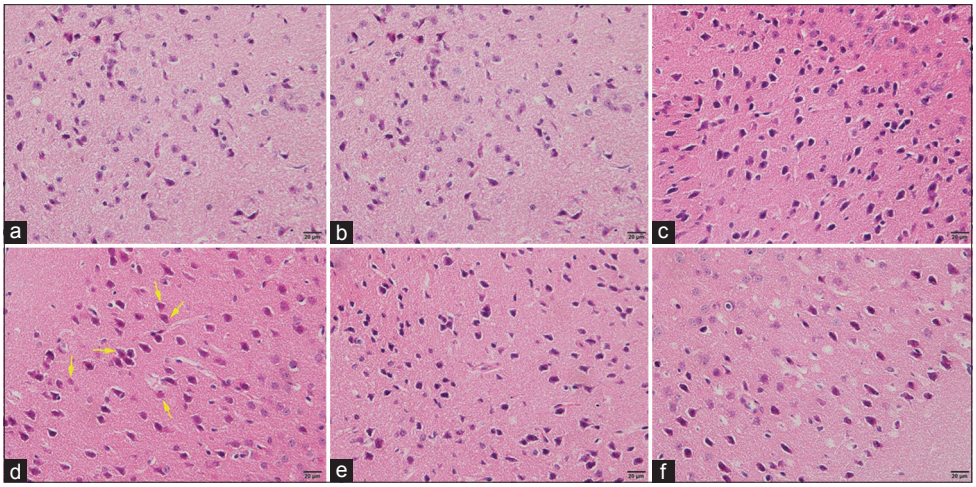

Figure 7: The frontal lobes of bTBI groups and sham bTBI group stained with H and E. Representative images of sham bTBI group (a) and bTBI 6-h, 1-day, 3-day, 7-day, and 14-day groups (b-f). The most significant necrotic cells were visible at 3 days (78 ± 8/HPF, $t = 6.1$, $P < 0.001$) after bTBI than sham group (2 ± 1/HPF). Yellow arrows indicate cytoplasmic acidification and rupture of the nuclear membrane. Scale bar = 20 μm. Data were presented as the mean ± standard error of the mean ($n = 6$ in each group). H and E: Hematoxylin and eosin; bTBI: Blast-induced traumatic brain injury; HPF: High-power field.

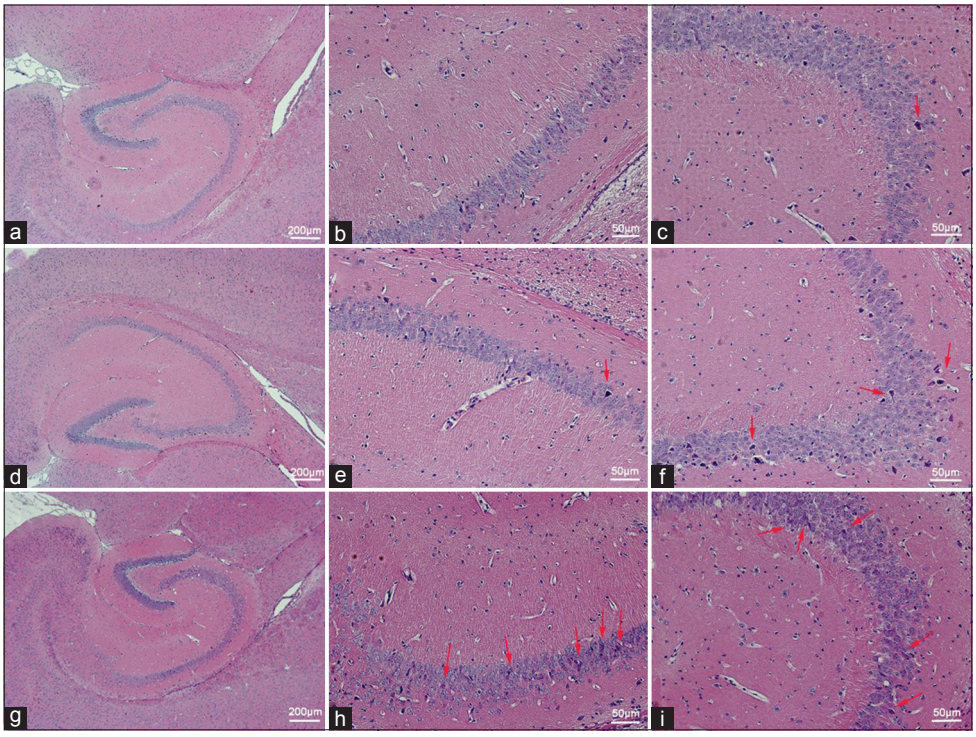

Figure 8: H and E stains in hippocampus of bTBI groups and sham bTBI group. Representative images of sham bTBI group (a-c) and bTBI 1-day (d-f) and 3-day groups (g-i). The bTBI 3-day group displayed more necrotic cells in CA1 and CA3 regions of the hippocampus (50 ± 5/HPF, $t = 16.3$, $P < 0.001$ and 40 ± 4/HPF, $t = 21.1$, $P < 0.001$) than the sham one (5 ± 2/HPF, and 2 ± 1/HPF). Red arrows indicate necrotic cells. Scale bar = 200 μm (a, d, and g), and scale bar = 50 μm (b, c, e, f, h, and i). Data were presented as the mean ± standard error of the mean ($n = 6$ in each group). H and E: Hematoxylin and eosin; bTBI: Blast-induced traumatic brain injury; HPF: High-power field.

and NeuN revealed TUNEL-positive apoptotic cells mainly in neurons. The apoptosis indexes of bTBI 1 day (25.06% ± 2.15% vs. 2.89% ± 0.84%, $t = 16.62$, $P = 0.004$) and bTBI 7-day group (6.11% ± 0.62% vs. 2.89% ± 0.84%, $t = 5.34$, $P = 0.031$) were higher than that of the sham bTBI group, and the apoptosis index of bTBI 3-day group was the highest (62.15% ± 3.24% vs. 2.89% ± 0.84%, $t = 30.64$, $P = 0.002$). Few TUNEL-positive apoptotic neurons were detected in the sham and bTBI 7-day groups. The apoptotic ratio of the total neurons in the frontal cortex was higher in bTBI 1-day group (4.50% ± 0.93% vs. 1.30% ± 0.11%, $t = 3.56$, $P = 0.007$) and was the most visible at 3 days post-bTBI (52.76% ± 1.99% vs. 1.30% ± 0.11%, $t = 57.20$, $P < 0.001$).

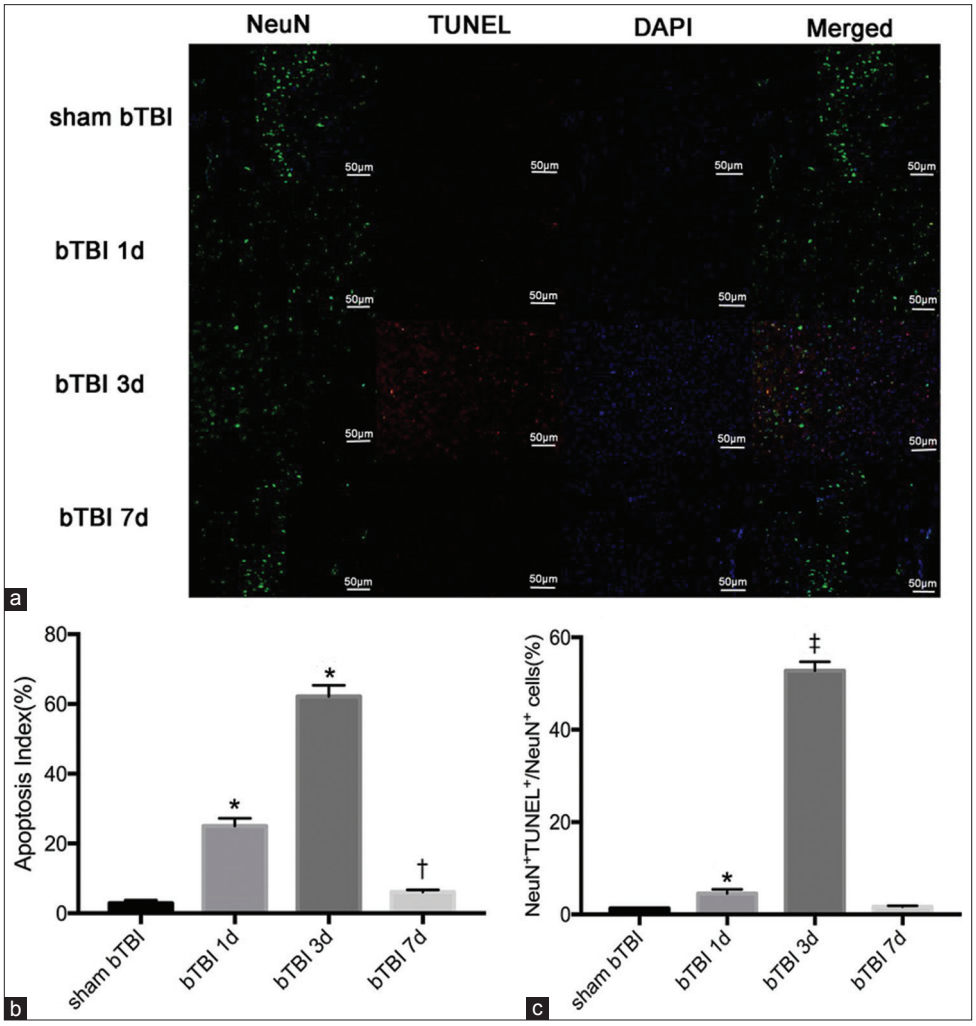

Figure 9: Apoptotic cells and neurons in the frontal lobe investigated through double staining of TUNEL and NeuN. (a) Representative fluorescence images of bTBI 1-day, 3-day, and 7-day groups and sham bTBI group. Fluorescence colors: TUNEL: Red, NeuN: Green, and DAPI: Blue. Scale bar = 50 μm. TUNEL and NeuN double-stained cells indicated the apoptotic neurons. (b) Quantitative analysis of apoptotic index in different groups. The apoptosis indexes of bTBI 1-day (25.06% ± 2.15% vs. 2.89% ± 0.84%, $t = 16.62$, $P = 0.004$) and bTBI 7-day group (6.11% ± 0.62% vs. 2.89% ± 0.84%, $t = 5.34$, $P = 0.031$) were higher than that of sham bTBI group, and the apoptosis index of bTBI 3-day group was the highest (62.15% ± 3.24% vs. 2.89% ± 0.84%, $t = 30.64$, $P = 0.002$). (c) Quantitative analysis of apoptotic neurons in different groups. Few TUNEL-positive apoptotic neurons were detected in the sham and bTBI 7-day groups. The apoptotic ratio of the total neurons in the frontal cortex was higher in bTBI 1-day group (4.50% ± 0.93% vs. 1.30% ± 0.11%, $t = 3.56$, $P = 0.007$) and was the most visible at 3 days post-bTBI (52.76% ± 1.99% vs. 1.30% ± 0.11%, $t = 57.20$, $P < 0.001$). Data were presented as the mean ± standard error of the mean ($n = 6$ in each group). *$P < 0.01$, †$P < 0.05$, ‡$P < 0.001$ compared with sham bTBI group. TUNEL: Terminal deoxynucleotidyl transferase-mediated dUTP nick 3'-end labeling; NeuN: Neuronal nuclei; bTBI: Blast-induced traumatic brain injury; DAPI: 4',6-diamidino-2-phenylindole.

Expression of glial fibrillary acidic protein is remarkably higher in the frontal lobe and hippocampus at 3 days after blast-induced traumatic brain injury induced by moderate intensity shock wave

Interface astroglial scarring at boundaries between brain parenchyma and fluids, and at junctions between gray and white matter, has been detected exclusively in blast-exposed brain specimens.[26] Here, the expression of GFAP determined the astrocyte activation after bTBI. Interestingly, GFAP positive expression was detected around the ventricles of the brain, around the blood vessels, and in the brainstem and hippocampus compared with sham bTBI group [Figure 10]. After bTBI, activated astrocytes in the frontal lobe began to rise significantly at 3 days [Figure 11; 2.98 ± 0.24 vs. 1.00 ± 0.00, $t = 14.42$, $P = 0.021$] and continued to rise at 7 days (4.23 ± 0.23 vs. 1.00 ± 0.00, $t = 23.87$, $P = 0.008$) and 14 days (5.33 ± 0.29 vs. 1.00 ± 0.00, $t = 26.10$, $P = 0.006$). However, the astrocyte activation in hippocampus demonstrated a multiphase pattern, in which after an immediate peak at 6 h (1.41 ± 0.09 vs. 1.00 ± 0.00, $t = 3.67$, $P = 0.003$), a period of relative decline at 1 day ensued followed by another peak expression at 3 days (1.70 ± 0.25 vs. 1.00 ± 0.00, $t = 6.24$, $P < 0.001$), and then decreased gradually at 7 days (1.67 ± 0.15 vs. 1.00 ± 0.00, $t = 5.93$, $P < 0.001$) and 14 days.

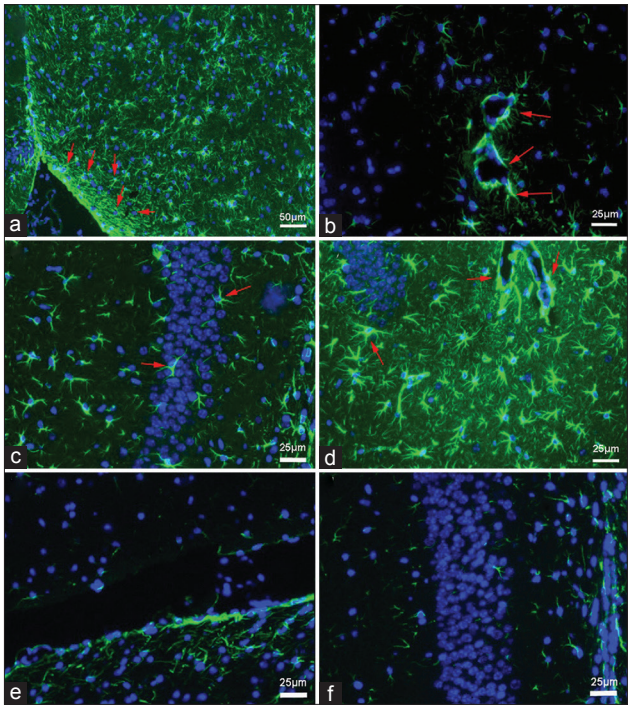

Figure 10: Representative merged GFAP fluorescence images of bTBI 3-day and sham bTBI groups. GFAP positive expression was noticed around the ventricles of the brain and in the brainstem (a). Much astrocyte activation was detected around the blood vessels (b) and in the hippocampus (c and d) as well. But in sham bTBI group, little GFAP positive expression was present around the ventricles of the brain (e) or in the hippocampus (f). Red arrows indicate the astrocyte activation. Fluorescence colors: GFAP: Green and DAPI: Blue. Scale bar = 50 μm (a), and scale bar = 25 μm (b-f). GFAP: Glial fibrillary acidic protein; bTBI: Blast-induced traumatic brain injury; DAPI: 4',6-diamidino-2-phenylindole.

Discussion

Most BINT research has focused on the mechanisms and effects of primary factors. With the improvement of the model, smaller volume, more convenient operation, and repeatability have become keys to the popularization of blast tests.[27-29] For this reason, we modified the indoor system referencing the previous models.[13,16,17] One change was the use of an electric gas pump instead of the conventional gas cylinder. The produced compressed air achieved the same effect as high-pressure helium or nitrogen gas released from the helium or nitrogen cylinder. Furthermore, the adaptation had the advantages of small size and increased safety. Another improvement was the combination of a traditional driven chamber with multiple holes to measure pressure and a driving chamber of matching flanges. The change measures the transmission and change of the shock wave in real time and miniaturizes the volume. Stainless steel, rather than aluminum, pipe was applied because of its higher strength and compressive strength. In each test, the whole body including head and neck of the mouse was fixed to the animal holder aiming to avoid tertiary injury. The shape and weight of animal holder with mesh ensured no displacement in each explosion. Torso shielding, which

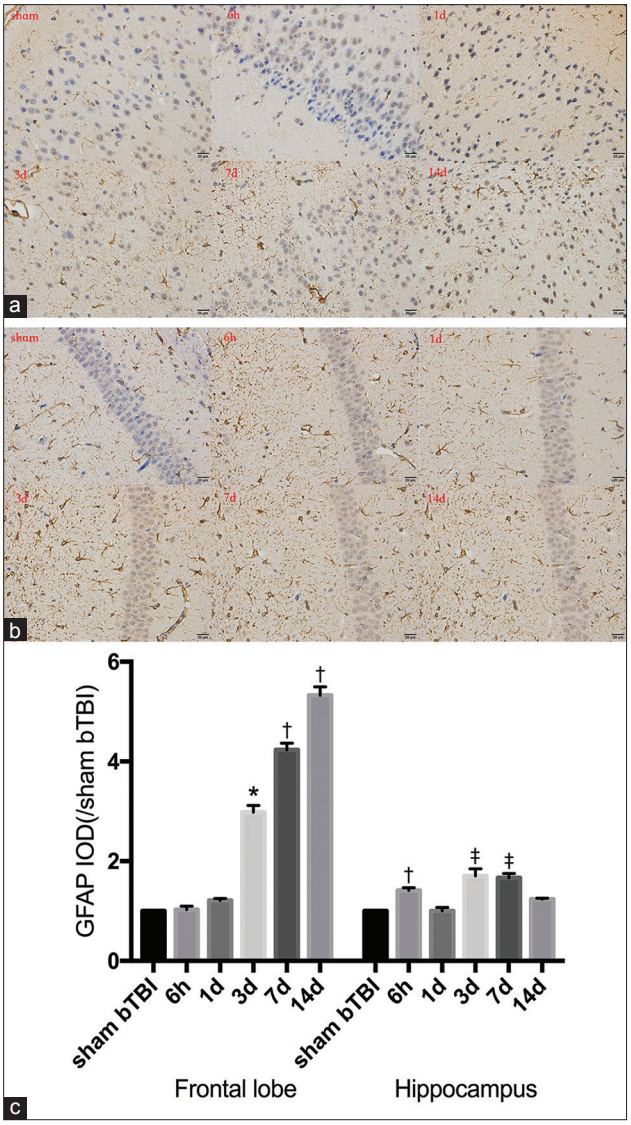

Figure 11: Immunohistochemistry of GFAP in the frontal lobe and hippocampus at 3 days after bTBI induced by moderate intensity shock wave. (a) Representative images of bTBI 6-h, 1-day, 3-day, 7-day, and 14-day groups and sham bTBI group in the frontal lobe. Scale bar = 20 μm. (b) Representative images of bTBI 6-h, 1-day, 3-day, 7-day, and 14-day groups and sham bTBI group in hippocampus. Scale bar = 20 μm. (c) Quantitative analysis of the astrocyte activation in the different groups. After bTBI, activated astrocytes in frontal lobe began to rise significantly at 3 days (2.98 ± 0.24 vs. 1.00 ± 0.00, $t = 14.42$, $P = 0.021$) and then continued to rise at 7 days (4.23 ± 0.23 vs. 1.00 ± 0.00, $t = 23.87$, $P = 0.008$) and 14 days (5.33 ± 0.29 vs. 1.00 ± 0.00, $t = 26.10$, $P = 0.006$). However, the astrocyte activation in hippocampus demonstrated a multiphase pattern, which meant after an immediate peak at 6 h (1.41 ± 0.09 vs. 1.00 ± 0.00, $t = 3.67$, $P = 0.003$), a period of relative decline at 1 day ensued followed by another peak expression at 3 days (1.70 ± 0.25 vs. 1.00 ± 0.00, $t = 6.24$, $P < 0.001$), and then decreased gradually at 7 days (1.67 ± 0.15 vs. 1.00 ± 0.00, $t = 5.93$, $P < 0.001$) and 14 days. Data were presented as the mean ± standard error of the mean ($n = 6$ in each group). *$P < 0.05$, †$P < 0.01$, ‡$P < 0.001$ compared with sham bTBI group. GFAP: Glial fibrillary acidic protein; IOD: Integrated optical density; bTBI: Blast-induced traumatic brain injury.

has been proven to be neuroprotective,[30] was used to protect the internal organs in each test. The driven length to diameter

ratio was greater than 10 to ensure the relatively planar shock wave.[10] Consistent with the previous literature, pressure time histories recorded at three pressure sensors were similar to the ideal Friedlander wave, and the measured shock wave speed approached the theoretical shock wave speed.[16] The duration of blast peak incident pressures at PS3 was <4 ms, which may accurately represent the exposures seen in BINT victims. This shock wave system was simple to use and stable because of its ability to produce repeatable blast waveforms that resemble free-field blast waves in a controlled laboratory environment.

Graded injury of BINT has been reported in other animal models.[29,31] In this study, we found that the modified shock tube system could successfully simulate mild, moderate, and severe graded intensity shock waves. The pressure ranges at PS3 of 170 ± 14 kPa, 236 ± 24 kPa, and 330 ± 27 kPa were referred to pressure generated by other established models in the literature.[13] The resulting injury from PTFE films of distinct thickness may be classified by value of PSS. Qualitative relationships between injury levels and PSS for the most commonly blast traumatized organs has been elucidated.[18] Here, we also observed discrepant mortality among graded blast. Most of the mice showed significant isolated parenchymal contusions or confluent hepatized regions encompassing areas ≥30% of the lung. Other organs, such as the pharynx/larynx, trachea, and hollow or solid abdominal organs, had not yet displayed significant damage. Mice exposed to moderate blast displayed a 5% mortality rate and isolated parenchymal contusions were evident in the lung, while none of mice in the mild blast group died. The limited mortality rate in the moderate group was caused by imminent cardiorespiratory arrest most probably due to vagovagal reflex activation as previously posited.[13] Similarly, the mortality and injury of mice increased with the increased pressure.[32]

At present, the most frequent symptoms of mice suffering moderate blast were malaise and anorexia, followed by incontinence, with apnea and seizure being less frequent. These acute presentations occurred within 3 days post-bTBI. Cardiopulmonary resuscitation has been used for apnea to reduce the death rate. Seizures have been reported in patients who have suffered blast injuries in the Global War on Terror.[33] The finding that explosive blast leads to consistent neuropathological brain changes raises significant concern that seizures and epilepsy may be more prevalent than previously suspected.[33,34] In our test, seizure was characterized by twitching in the extremities, which may correlate with potential brain damage.

Development of subarachnoid hemorrhage, brain edema, hyperemia, and delayed vasospasm are very common for the patients suffering from moderate to severe bTBI. Analogously, subarachnoid hemorrhage and brain edema were detected both by CT scan and gross observation. Further detection of the brain water content confirmed that brain edema was the most serious at 3 days post-bTBI. Isolated parenchymal contusions were noticeable in lung; lung damage may contribute to the brain injury. However, the specific mechanism has not yet been clarified. No focal lesions, contusion, or cerebral hematoma were presently evident after blast. This may be the result of mild-to-moderate blast damage to the brain. The BBB was not disrupted, probably because single injury had no significant effect, as has been reported.[35]

In our model, mice displayed the worst functional outcome at 1 day post-bTBI induced by moderate explosion. The slightly modified point in NSS reflected paresis of the upper and/or lower limbs of one lateral side, rather than the contralateral side, simply because the injured side of frontal lobe was uncertain. The righting reflex time, as an indicator of early neurologic injury, can be significantly prolonged following moderate blast.[36] Gross examination of the limbs after blast showed no physical injury, indicating that extremity injury was not the reason for the delayed righting reflex time. Spatial memory and motor activity abnormalities were observed obviously at 1 day post-bTBI, perhaps reflecting the pathophysiology of bTBI. This speculation requires further research.

Histopathology examination was done to illuminate the probable pathological mechanism underlying long-term neurological impairments. In general, neuronal, axonal, and glial injuries have all been observed following single-blast exposure.[26,37-39] H and E staining indicated the most necrotic cells in the frontal lobe and hippocampus at 3 days after bTBI induced by moderate intensity shock wave. Interestingly, TUNEL and NeuN double staining showed that apoptotic neurons in the frontal cortex peaked at 3 days after bTBI. Both apoptotic and necrotic pathways appear to contribute to neuronal death.[40] Acute axonal injury was not yet prominent, maybe because the tertiary effect in our model was mild. The peak of neuronal apoptosis at 3 days post-bTBI may be due to the mechanism of shock wave injury, strength of damage, and gradual neuron death.[13,33] The affected frontal cortex and hippocampus can be linked to impaired behavior. GFAP immunoreactivity reveals neocortical tissue in the initial stages of GFAP deposition, indicating early repair response.[32] Reactive astrogliosis has been established as one of the key components of the cellular response to brain injury.[41] Our data as well as that of others reveal GFAP positive expression at boundaries between brain parenchyma and fluids, which may indicate specific areas of damage from blast exposure, which is consistent with the general principles of blast biophysics.[26] We identified different trends of glial activation between the frontal lobe and hippocampus. After bTBI, the expression of GFAP in the frontal lobe was the highest at 3 days and then continued to rise, while two peaks appeared in the hippocampus at 6 h and 3 days, and then declined gradually. This tendency of two peaks is consistent with a previous finding.[13] Reactive gliosis and neuronal swelling also have been observed in the hippocampus of rats subjected to blast injury.[42] Overall, neuronal injury and gliosis in frontal lobe and hippocampus were significantly higher at 3 days post-bTBI induced by moderate blast. Previously, exposure to primary blast alone

resulted in changes in hippocampus-dependent behaviors that corresponded with electrophysiological changes in area CA1 accompanied by reactive gliosis.[43] Astrocytes have also been implicated in brain and neuronal functions supporting learning and memory and emotional responses.[44] In our study, impaired behavior was the most severe at 1 day after bTBI and gradually diminished with the enhancement of GFAP activity. The relationship between GFAP activity and behavior may be implied.

In summary, a modified bTBI model in mice has been developed to generate a physical environment similar to the battlefield. The data showed that a graded intensity shock wave blast can be simulated, and after moderate blast, the alterations in clinical manifestation, imaging manifestation, neuroethology, and neuropathology are comparable with the performance of mild-to-moderate bTBI. The modified blast tube model may offer some advantages for studying the mechanism of bTBI and its treatment.

Financial support and sponsorship

This work was supported by grants from the Youth Training Project (No. 16QNP042), the Medical and Health Scientific Research Fund by Nanjing Military Region (No. ZX28), and the Jinling Hospital of Nanjing (No. 2016017).

Conflicts of interest

There are no conflicts of interest.

References

1. Newsome MR, Mayer AR, Lin X, Troyanskaya M, Jackson GR, Scheibel RS, *et al.* Chronic effects of blast-related TBI on subcortical functional connectivity in veterans. J Int Neuropsychol Soc 2016;22:631-42. doi: 10.1017/S1355617716000448.
2. Ropper A. Brain injuries from blasts. N Engl J Med 2011;364:2156-7. doi: 10.1056/NEJMe1102187.
3. Dams-O'Connor K, Tsao JW. Functional decline 5 years after blast traumatic brain injury: Sounding the alarm for a wave of disability? JAMA Neurol 2017;74:763-4. doi: 10.1001/jamaneurol.2017.0176.
4. Bowen LN, Moore DF, Okun MS. Is blast injury a modern phenomenon?: Early historical descriptions of mining and volcanic traumatic brain injury with relevance to modern terrorist attacks and military warfare. Neurologist 2016;21:19-22. doi: 10.1097/NRL.0000000000000068.
5. Schindler AG, Meabon JS, Pagulayan KF, Hendrickson RC, Meeker KD, Cline M, *et al.* Blast-related disinhibition and risk seeking in mice and combat veterans: Potential role for dysfunctional phasic dopamine release. Neurobiol Dis 2017;106:23-34. doi: 10.1016/j.nbd.2017.06.004.
6. Cernak I. Blast injuries and blast-induced neurotrauma: Overview of pathophysiology and experimental knowledge models and findings. In: Kobeissy FH, editor. Brain Neurotrauma: Molecular, Neuropsychological, and Rehabilitation Aspects. Boca Raton (FL): CRC Press/Taylor and Francis; 2015.
7. Lesperance RN, Nunez TC. Blast injury: Impact on brain and internal organs. Crit Care Nurs Clin North Am 2015;27:277-87. doi: 10.1016/j.cnc.2015.02.007.
8. Ling G, Ecklund JM, Bandak FA. Brain injury from explosive blast: Description and clinical management. Handb Clin Neurol 2015;127:173-80. doi: 10.1016/B978-0-444-52892-6.00011-8.
9. Rafaels KA, Bass CR, Panzer MB, Salzar RS, Woods WA, Feldman SH, *et al.* Brain injury risk from primary blast. J Trauma Acute Care Surg 2012;73:895-901. doi: 10.1097/TA.0b013e31825a760e.
10. Bass CR, Panzer MB, Rafaels KA, Wood G, Shridharani J, Capehart B, *et al.* Brain injuries from blast. Ann Biomed Eng 2012;40:185-202. doi: 10.1007/s10439-011-0424-0.
11. Risling M, Davidsson J. Experimental animal models for studies on the mechanisms of blast-induced neurotrauma. Front Neurol 2012;3:30. doi: 10.3389/fneur.2012.00030.
12. Courtney A, Courtney M. The complexity of biomechanics causing primary blast-induced traumatic brain injury: A Review of potential mechanisms. Front Neurol 2015;6:221. doi: 10.3389/fneur.2015.00221.
13. Cernak I, Merkle AC, Koliatsos VE, Bilik JM, Luong QT, Mahota TM, *et al.* The pathobiology of blast injuries and blast-induced neurotrauma as identified using a new experimental model of injury in mice. Neurobiol Dis 2011;41:538-51. doi: 10.1016/j.nbd.2010.10.025.
14. Long JB, Bentley TL, Wessner KA, Cerone C, Sweeney S, Bauman RA, *et al.* Blast overpressure in rats: Recreating a battlefield injury in the laboratory. J Neurotrauma 2009;26:827-40. doi: 10.1089/neu.2008.0748.
15. Wang Y, Sawyer TW, Tse YC, Fan C, Hennes G, Barnes J, *et al.* Primary blast-induced changes in akt and GSK3β phosphorylation in rat hippocampus. Front Neurol 2017;8:413. doi: 10.3389/fneur.2017.00413.
16. Panzer MB, Matthews KA, Yu AW, Morrison B 3rd, Meaney DF, Bass CR, *et al.* A multiscale approach to blast neurotrauma modeling: Part I – development of novel test devices for *in vivo* and *in vitro* blast injury models. Front Neurol 2012;3:46. doi: 10.3389/fneur.2012.00046.
17. Koliatsos VE, Cernak I, Xu L, Song Y, Savonenko A, Crain BJ, *et al.* A mouse model of blast injury to brain: Initial pathological, neuropathological, and behavioral characterization. J Neuropathol Exp Neurol 2011;70:399-416. doi: 10.1097/NEN.0b013e3182189f06.
18. Yelveton JT. Pathology scoring system for blast injuries. J Trauma 1996;40:S111-5. doi: 10.1097/00005373-199603001-00025.
19. Zhang L, Wang H, Fan Y, Gao Y, Li X, Hu Z, *et al.* Fucoxanthin provides neuroprotection in models of traumatic brain injury via the nrf2-ARE and nrf2-autophagy pathways. Sci Rep 2017;7:46763. doi: 10.1038/srep46763.
20. Koyama Y, Andoh T, Kamiya Y, Miyazaki T, Maruyama K, Kariya T, *et al.* Bumetanide, an inhibitor of NKCC1 (Na-K-2Cl cotransporter isoform 1), enhances propofol-induced loss of righting reflex but not its immobilizing actions in neonatal rats. PLoS One 2016;11:e0164125. doi: 10.1371/journal.pone.0164125.
21. Abdulbasit A, Stephen Michael F, Shukurat Onaopemipo A, Abdulmusawwir AO, Aminu I, Nnaemeka Tobechukwu A, *et al.* Glucocorticoid receptor activation selectively influence performance of wistar rats in Y-maze. Pathophysiology 2018;25:41-50. doi: 10.1016/j.pathophys.2017.12.002.
22. Zhang L, Ding K, Wang H, Wu Y, Xu J. Traumatic brain injury-induced neuronal apoptosis is reduced through modulation of PI3K and autophagy pathways in mouse by FTY720. Cell Mol Neurobiol 2016;36:131-42. doi: 10.1007/s10571-015-0227-1.
23. Li T, Sun KJ, Wang HD, Zhou ML, Ding K, Lu XY, *et al.* Tert-butylhydroquinone ameliorates early brain injury after experimental subarachnoid hemorrhage in mice by enhancing Nrf2-independent autophagy. Neurochem Res 2015;40:1829-38. doi: 10.1007/s11064-015-1672-4.
24. Fang XX, Sun GL, Zhou Y, Qiu YH, Peng YP. TGF-β1 protection against aβ1-42-induced hippocampal neuronal inflammation and apoptosis by tβR-I. Neuroreport 2018;29:141-6. doi: 10.1097/WNR.0000000000000940.
25. Ding K, Xu J, Wang H, Zhang L, Wu Y, Li T, *et al.* Melatonin protects the brain from apoptosis by enhancement of autophagy after traumatic brain injury in mice. Neurochem Int 2015;91:46-54. doi: 10.1016/j.neuint.2015.10.008.
26. Shively SB, Horkayne-Szakaly I, Jones RV, Kelly JP, Armstrong RC, Perl DP, *et al.* Characterisation of interface astroglial scarring in the human brain after blast exposure: A post-mortem case series. Lancet Neurol 2016;15:944-53. doi: 10.1016/S1474-4422(16)30057-6.
27. Genovese RF, Simmons LP, Ahlers ST, Maudlin-Jeronimo E, Dave JR, Boutte AM, *et al.* Effects of mild TBI from repeated blast overpressure on the expression and extinction of conditioned fear in rats. Neuroscience 2013;254:120-9. doi: 10.1016/j.neuroscience.2013.09.021.

28. del Mar N, von Buttlar X, Yu AS, Guley NH, Reiner A, Honig MG, *et al.* A novel closed-body model of spinal cord injury caused by high-pressure air blasts produces extensive axonal injury and motor impairments. Exp Neurol 2015;271:53-71. doi: 10.1016/j.expneurol.2015.04.023.
29. Mishra V, Skotak M, Schuetz H, Heller A, Haorah J, Chandra N, *et al.* Primary blast causes mild, moderate, severe and lethal TBI with increasing blast overpressures: Experimental rat injury model. Sci Rep 2016;6:26992. doi: 10.1038/srep26992.
30. Parisian CM, Georgevitch G, Bahr BA. Military blast-induced synaptic changes with distinct vulnerability may explain behavioral alterations in the absence of obvious brain damage. J Nat Sci 2017;3: e406.
31. Perez-Polo JR, Rea HC, Johnson KM, Parsley MA, Unabia GC, Xu GY, *et al.* A rodent model of mild traumatic brain blast injury. J Neurosci Res 2015;93:549-61. doi: 10.1002/jnr.23513.
32. Xu L, Schaefer ML, Linville RM, Aggarwal A, Mbuguiro W, Wester BA, *et al.* Neuroinflammation in primary blast neurotrauma: Time course and prevention by torso shielding. Exp Neurol 2016;277:268-74. doi: 10.1016/j.expneurol.2016.01.010.
33. Kovacs SK, Leonessa F, Ling GS. Blast TBI models, neuropathology, and implications for seizure risk. Front Neurol 2014;5:47. doi: 10.3389/fneur.2014.00047.
34. Luethcke CA, Bryan CJ, Morrow CE, Isler WC. Comparison of concussive symptoms, cognitive performance, and psychological symptoms between acute blast-versus nonblast-induced mild traumatic brain injury. J Int Neuropsychol Soc 2011;17:36-45. doi: 10.1017/S1355617710001207.
35. Wang Y, Wei Y, Oguntayo S, Wilkins W, Arun P, Valiyaveettil M, *et al.* Tightly coupled repetitive blast-induced traumatic brain injury: Development and characterization in mice. J Neurotrauma 2011;28:2171-83. doi: 10.1089/neu.2011.1990.
36. Kane MJ, Angoa-Pérez M, Briggs DI, Viano DC, Kreipke CW, Kuhn DM, *et al.* A mouse model of human repetitive mild traumatic brain injury. J Neurosci Methods 2012;203:41-9. doi: 10.1016/j.jneumeth.2011.09.003.
37. Yin TC, Voorhees JR, Genova RM, Davis KC, Madison AM, Britt JK, *et al.* Acute axonal degeneration drives development of cognitive, motor, and visual deficits after blast-mediated traumatic brain injury in mice. eNeuro 2016;3: ENEURO.0220-16.2016. doi: 10.1523/ENEURO.0220-16.2016.
38. Canchi S, Sarntinoranont M, Hong Y, Flint JJ, Subhash G, King MA, *et al.* Simulated blast overpressure induces specific astrocyte injury in an *ex vivo* brain slice model. PLoS One 2017;12:e0175396. doi: 10.1371/journal.pone.0175396.
39. Zander NE, Piehler T, Banton R, Benjamin R. Effects of repetitive low-pressure explosive blast on primary neurons and mixed cultures. J Neurosci Res 2016;94:827-36. doi: 10.1002/jnr.23786.
40. Hicks RR, Fertig SJ, Desrocher RE, Koroshetz WJ, Pancrazio JJ. Neurological effects of blast injury. J Trauma 2010;68:1257-63. doi: 10.1097/TA.0b013e3181d8956d.
41. Miller AP, Shah AS, Aperi BV, Kurpad SN, Stemper BD, Glavaski-Joksimovic A, *et al.* Acute death of astrocytes in blast-exposed rat organotypic hippocampal slice cultures. PLoS One 2017;12:e0173167. doi: 10.1371/journal.pone.0173167.
42. Dalle Lucca JJ, Chavko M, Dubick MA, Adeeb S, Falabella MJ, Slack JL, *et al.* Blast-induced moderate neurotrauma (BINT) elicits early complement activation and tumor necrosis factor α (TNFα) release in a rat brain. J Neurol Sci 2012;318:146-54. doi: 10.1016/j.jns.2012.02.002.
43. Beamer M, Tummala SR, Gullotti D, Kopil C, Gorka S, Abel T, *et al.* Primary blast injury causes cognitive impairments and hippocampal circuit alterations. Exp Neurol 2016;283:16-28. doi: 10.1016/j.expneurol.2016.05.025.
44. Perez-Urrutia N, Mendoza C, Alvarez-Ricartes N, Oliveros-Matus P, Echeverria F, Grizzell JA, *et al.* Intranasal cotinine improves memory, and reduces depressive-like behavior, and GFAP+ cells loss induced by restraint stress in mice. Exp Neurol 2017;295:211-21. doi: 10.1016/j.expneurol.2017.06.016.

使用一种改良的冲击波爆炸模型研究中等强度爆炸冲击波对小鼠的脑损伤

摘要

背景：随着爆炸伤的日益增多，对爆炸性脑损伤（bTBI）的关注也越来越多，很多研究通过不同的冲击波管道模型研究爆炸性脑损伤。轻中强度的爆炸往往因为症状出现慢或轻而容易忽视。然而，我们发现在现有的模型中使用的重型气瓶和大容量腔室可能会增加操作的复杂性和危险性。本研究旨在设计一种方便而安全的小鼠冲击波管道爆炸伤模型，同时研究中强度的爆炸对小鼠脑损伤的影响。

方法：使用病理评分系统(PSS)区分改良的小鼠冲击波管道模型制造的轻中重度的爆炸强度。总共160只小鼠随机分为空白组、假爆炸组、爆炸后不同时间点组，我们观察了中等强度的爆炸致bTBI后小鼠的临床症状、影像学表现、神经行为学和神经病理学的变化。我们用单因素方差分析联合Fisher's LSD检验或Dunnett-t3检验来比较各组数据间的差异。

结果：轻中重强度的冲击波对应的PSS分别为13.4±2.2、32.6±2.7(t=13.92, P<0.001)和56.6±2.8 (t=31.37, P<0.001)。遭受中等强度的冲击波刺激后，小鼠表现为不同程度的萎靡不振、厌食、尿失禁、呼吸暂停和癫痫。与假爆炸组相比，bTBI后3天脑水肿达到高峰(82.5±2.1% vs. 73.8±0.6%, t=7.76, P<0.001)，而bTBI后1天神经行为损伤最严重(Y迷宫：8.25±2.36 vs. 20.00±4.55, t=-4.59, P=0.048; 29.58±2.84% vs. 49.09±11.63%, t=-3.08, P=0.008; 神经严重程度评分：2.50±0.58 vs. 0.00±0.00, t=8.65, P=0.016)。同时我们发现，额叶的凋亡的神经元 (52.76±1.99% vs. 1.30±0.11%, t=57.20, P<0.001)和神经胶质增生(2.98±0.24 vs. 1.00±0.00, t=14.42, P=0.021)在bTBI后3天明显多于假爆炸组。

结论：我们改良了一种可靠的、重复性好的小鼠bTBI模型，能够在可控的实验室环境下产生类似于自由场冲击波的分级的爆炸波形；中等强度的爆炸冲击波可能导致了小鼠轻中度的脑损伤。